Journal of Visualized Experiments

Live Cell Imaging and Cryo-Electron Tomography to Resolve Spatiotemporal Features of the Legionella pneumophila Dot/Icm Secretion System

--Manuscript Draft--

Article Type:	Invited Methods Article - JoVE Produced Video
Manuscript Number:	JoVE60693R1
Full Title:	Live Cell Imaging and Cryo-Electron Tomography to Resolve Spatiotemporal Features of the Legionella pneumophila Dot/Icm Secretion System
Section/Category:	JoVE Biology
Keywords:	Legionella pneumophila, Type IV secretion system, Live cell imaging, Cryo-Electron Tomography
Corresponding Author:	David Chetrit Yale University School of Medicine New Haven, CT UNITED STATES
Corresponding Author's Institution:	Yale University School of Medicine
Corresponding Author E-Mail:	david.chetrit@yale.edu
Order of Authors:	David Chetrit
	Donghyun Park
	Bo Hu
	Jun Liu
	Craig Roy
Additional Information:	
Question	**Response**
Please indicate whether this article will be Standard Access or Open Access.	Standard Access (US$2,400)
Please indicate the **city, state/province, and country** where this article will be **filmed**. Please do not use abbreviations.	New Haven, Connecticut, USA

Yale SCHOOL OF MEDICINE

Department of Microbial Pathogenesis

David Chetrit, PHD

david.chetrit@yale.edu
C 203 764-0457
T 203 737-2409
Boyer Center for Molecular Medicine
Room 347
295 Congress Avenue
New Haven, CT 06536-0812

October 27, 2019

Phillip Steindel, Ph.D

Review Editor

Journal of Visualized Experiments

1 Alewife center

Cambridge, MA

Dear Dr. Steindel,

We have enclosed a revised version of manuscript JoVE60693 entitled, “Applying Live Cell Imaging and Cryo Electron Tomography to Resolve Spatiotemporal Features of the *Legionella pneumophila* Dot/Icm Secretion System”. We believe that all concerns have been addressed, as we have detailed in the point-by-point rebuttal to the editorial and reviewers comments.

We thank you for considering this manuscript for publication in Journal of Visualized Experiments and look forward to your decision.

Sincerely,

David Chetrit

David Chetrit, Ph.D.

Yale University School of Medicine

TITLE:

Live Cell Imaging and Cryo-Electron Tomography to Resolve Spatiotemporal Features of the *Legionella pneumophila* Dot/Icm Secretion System

AUTHORS AND AFFILIATIONS:

David Chetrit[1], Donghyun Park[1,2], Bo Hu[3], Jun Liu[1,2], Craig R. Roy[1]

[1]Department of Microbial Pathogenesis, Microbial Sciences Institute and Boyer Center for Molecular Medicine, Yale School of Medicine, New Haven, CT, USA
[2]Microbial Sciences Institute, Yale University, West Haven, CT, USA
[3]Department of Microbiology and Molecular Genetics, McGovern Medical School, The University of Texas Health Science Center at Houston, Houston, TX, USA.

Corresponding Author:

David Chetrit (david.chetrit@yale.edu)

Email Addresses of Co-authors:

Donghyun Park (donghyun.park@yale.edu)
Bo Hu (Bo.Hu@uth.tmc.edu)
Jun Liu (jliu@yale.edu)
Craig R. Roy (craig.roy@yale.edu)

KEYWORDS:

Legionella pneumophila, Legionnaires' disease, respiratory infection, intracellular bacterial pathogens, type IV secretion system, Dot/Icm secretion system, live cell imaging, spatiotemporal dynamics, quantitative fluorescence microscopy, cryo-electron tomography, cellular structures, allelic exchange

SUMMARY:

Imaging of bacterial cells is an emerging systems biology approach focused on defining static and dynamic processes that dictate the function of large macromolecular machines. Here, integration of quantitative live cell imaging and cryo-electron tomography is used to study *Legionella pneumophila* type IV secretion system architecture and functions.

ABSTRACT:

The Dot/Icm secretion system of *Legionella pneumophila* is a complex type IV secretion system (T4SS) nanomachine that localizes at the bacterial pole and mediates the delivery of protein and DNA substrates to target cells, a process generally requiring direct cell-to-cell contact. We have recently solved the structure of the Dot/Icm apparatus by cryo-electron tomography (cryo-ET) and showed that it forms a cell envelope-spanning channel that connects to a cytoplasmic complex. Applying two complementary approaches that preserve the native structure of the specimen, fluorescent microscopy in living cells and cryo-ET, allows in situ visualization of proteins and assimilation of the stoichiometry and timing of production of each machine component relative to other Dot/Icm subunits. To investigate the requirements for polar

positioning and to characterize dynamic features associated with T4SS machine biogenesis, we have fused a gene encoding superfolder green fluorescent protein to Dot/Icm ATPase genes at their native positions on the chromosome. The following method integrates quantitative fluorescence microscopy of living cells and cryo-ET to quantify polar localization, dynamics, and structure of these proteins in intact bacterial cells. Applying these approaches for studying the *Legionella pneumophila* T4SS is useful for characterizing the function of the Dot/Icm system and can be adapted to study a wide variety of bacterial pathogens that utilize the T4SS or other types of bacterial secretion complexes.

INTRODUCTION:

Legionella pneumophila (*L. pneumophila*), the etiological agent of Legionnaires' disease, inhabits freshwater reservoirs, where the bacteria propagate by infecting and replicating within aquatic free-swimming protozoa. *L. pneumophila* causes disease outbreaks in humans when inhalation of aerosolized bacteria from potable water sources occurs. In infected cells, subversion of host pathways allows *L. pneumophila* to delay endocytic maturation of the vacuole in which it resides and to promote biogenesis of a cellular compartment that supports bacterial replication. This process is driven by a specialized bacterial type IVB secretion system (T4BSS) known as Dot/Icm and its repertoire of over 300 "effector" proteins that are translocated into the host cytosol during infection to facilitate manipulation of cellular functions[1–5]. Mutants lacking a functional Dot/Icm apparatus fail to deliver effectors into the host cytosol, are defective for intracellular replication, and are avirulent in animal models of disease[6,7].

Many bacterial species have developed extremely complex and dynamic multicomponent machines that are required for infection processes. Other T4BSS like the Dot/Icm system are also essential for intracellular replication of bacterial pathogens such as *Coxiella burnetii* and *Rickettsiella grylli*. Although T4BSS are evolutionarily related to prototypical type IVA systems, which mediate DNA transfer and can deliver a limited repertoire of effector proteins, the Dot/Icm system has nearly twice as many machine components and delivers a wide variety of effectors. Presumably, this expansion in the number of components has enabled the Dot/Icm apparatus to accommodate and integrate new effectors easily[8,9].

We recently used cryo-electron tomography (cryo-ET) to solve the structure of the Dot/Icm apparatus in situ and showed that it forms a cell envelope-spanning channel that connects to a cytoplasmic complex. Further analysis revealed that the cytosolic ATPase DotB associates with the Dot/Icm system at the *L. pneumophila* cell pole through interactions with the cytosolic ATPase DotO. We have discovered that DotB displays a cytosolic movement in most bacterial cells, indicating that this ATPase is present in a dynamic cytosolic population but also associates with the polar Dot/Icm complexes. In addition, DotO forms a hexameric assembly of DotO dimers associated with the inner membrane complex, and a DotB hexamer joins to the base of this cytoplasmic complex. The assembly of the DotB-DotO energy complex creates a cytoplasmic channel that directs the translocation of substrates through the T4SS (**Figure 1**)[10].

Despite these recent advances, little is known about how the Dot/Icm system functions and how each protein assembles to form an active apparatus[8]. Uncovering the regulatory circuitry of the

Dot/Icm T4SS is fundamental to understanding the molecular mechanisms of host-pathogen interactions. Therefore, we discuss how to use live cell microscopy and cryo-ET to detect and characterize essential *L. pneumophila* Dot/Icm system components that are tagged with super-folder GFP (sfGFP). Using quantitative fluorescence microscopy, the polar localization of DotB will be defined in a wild type background or when the type IV system is deleted. Time-lapse microscopy will be used to quantify differences in localization and dynamics between the Dot/Icm cytosolic ATPases.

The combined application of two complementary approaches such as live imaging and cryo-ET provides an advantage compared to other in vitro systems. Both methods are performed in intact cells and preserve the natural environment of the T4BSS, thus minimizing disruption of the native structure during sample preparation. Because overexpression of proteins may impair the stoichiometry of the secretion apparatus, sfGFP fusions are returned via allelic exchange to the *Legionella* chromosome so that each fusion is encoded in single copy and the expression is driven by the endogenous promoter. Visualization of chromosomally-encoded fusions enables quantification of the exact level of protein being expressed at a defined time point. Cryo-ET also has many advantages for determining the structure of secretion systems. The most notable advantage is that cryo-ET samples are comprised of frozen intact cells that preserve native complexes in the context of bacterial cell architecture. Consequently, cryo-ET may be preferable to biochemical purification approaches, which extract membrane complexes and may strip peripheral proteins from the core apparatus or modify the overall structure. In addition, tagging a protein of interest with a bulky protein such as sfGFP adds a mass that is detectable by cryo-ET and can assist with mapping the different subcomplexes of the Dot/Icm apparatus onto the structure obtained by cryo-ET.

This approach is a powerful tool for uncovering structural information about multimolecular complexes that assemble in the bacterial cell membrane. The interpretation of structures elucidated using these techniques will help the field understand how T4BSS components function, why so many components are required for function, how the components interact within the greater complex, and what functions these subassemblies perform.

PROTOCOL:

NOTE: All procedures involving the growth, manipulation, and imaging of *L. pneumophila* should be performed in a Physical Containment Level 2 Laboratory and within a biological safety cabinet in compliance with local guidelines.

1. Insertion of sfGFP into *L. pneumophila* chromosome using allelic exchange and double selection strategy (Figure 2, Figure 3)

1.1. Clone into the gene replacement vector pSR47S[11] the following sequence: the 1,000 bp upstream of the site of interest, then the sfGFP sequence, then the 1,000 bp downstream of the site of interest (**Figure 2**). The sfGFP sequence should be placed in frame to the N-terminus or C-terminus ends with a linker that contains four to eight amino acids. Transform the resulting

vector into *E. coli* DH5αλpir. Later, streak *L. pneumophila* (the recipient) for single colonies on charcoal-yeast extract (CYE) agar[12] containing 100 µg/mL streptomycin and grow for 5 days at 37 °C (**Figure 3**).

1.2. Streak *L. pneumophila* on CYE-agar-streptomycin and grow for 2 days at 37 °C (heavy patch)[10]. Streak *E. coli* DH5α transformed with pRK600 helper plasmid (helper)[13] on LB agar containing 25 µg/mL chloramphenicol. Streak the *E. coli* DH5αλpir (donor) on LB agar containing 50 µg/mL kanamycin.

1.3. Perform triparental mating: incubate a colony of the helper, a colony of the donor, and the recipient by overlaying patches of the three strains on a CYE agar plate without selection and incubating for 4–8 hours at 37 °C. As negative controls incubate a helper+recipient strain mix and a donor+recipient strain mix for the same periods of time.

1.4. Resuspend the mating reactions in 500 µL of ddH_2O. Plate 20 µL and 50 µL of the reactions on CYE agar containing 100 µg/mL streptomycin and 10 µg/mL kanamycin and grow for 5 days at 37 °C. Streak four of the resulting clones on CYE agar containing 100 µg/mL streptomycin and grow for 5 days at 37 °C.

1.5. Streak 16 clones on CYE agar containing 5% sucrose and 100 µg/mL streptomycin and grow for 5 days at 37 °C. Then, streak 32 of these clones on CYE agar containing 100 µg/mL streptomycin and on CYE agar containing 100 µg/mL streptomycin and 10 µg/mL kanamycin and grow for 5 days at 37 °C.

2. Isolation of clones that integrated sfGFP into the *L. pneumophila* chromosome

2.1. Streak clones that were sensitive to kanamycin on CYE-agar-streptomycin plates and confirm the insertion of sfGFP into the chromosome with colony PCR. Use primers that are complementary to the sfGFP gene and to the chromosomal region of interest to amplify the insertion junction.

2.1.1. Mix 0.5 µL of each of the 10 µM primers solutions and one colony to a final volume of 12.5 µL and denature for 10 min at 95 °C. Cool on ice for 10 min, add 12.5 µL of 2x PCR master mix solution, and perform a PCR analysis.

2.2. Grow heavy patches of the isolated colonies on CYE-agar-streptomycin plates for 2 days at 37 °C. Examine the expression levels and stability of the sfGFP fusions by immunoblotting with an anti-GFP antibody.

3. Live cell imaging of *L. pneumophila* with fluorescently tagged Dot/Icm components

3.1. Preparation of agarose pads

3.1.1. Make about 30 mL of a 1% low-melt agarose solution in water. Microwave in a glass flask

for about 90 s, swirling occasionally, until the agarose is completely dissolved.

3.1.2. Place two 22 x 22 x 0.15 mm glass slides on the edge of a 25 x 75 x 1.1 mm glass slide, one on top of the other. Stack two more 22 x 22 x 0.15 mm glass slides on the other edge.

3.1.3. Pipette about 1 mL of the molten agarose into the center slide between the two upper glass slides, then place another 25 x 75 x 1.1 mm slide on top of the molten agarose. Try to avoid the formation of air bubbles. Cool the slides at 4 °C for 15 min.

3.1.4. Using a scalpel or razor blade, gently cut the pad into small squares, ~5 x 5 mm. Fix a double-sided adhesive 17 x 28 x 0.25 mm frame on a 25 x 75 x 1.1 mm glass slide and place several pads on the slide.

3.2. Image acquisition

Note: The following steps are described for a microscope that is under the control of SlideBook 6.0 and equipped with solid state illuminators, CCD monochrome camera, and a 100x objective lens (1.4 numerical aperture). If needed, use alternative microscopy devices with appropriate hardware and software configurations that can be customized according to the protocol settings.

3.2.1. Dissolve a heavy patch of *L. pneumophila* in 1 mL of ddH_2O, vortex and pipet 2–3 µL of the dilution onto the pads. Place a 50 x 24 x 0.15 mm coverslip gently over the adhesive frame.

3.2.2. In the capture window adjust the ND to 180. Adjust the binning to 2×2 and use the 488 nm channel to expose the sample between 500–1,000 ms. Validate the specificity of the fluorescence signal by imaging untagged *L. pneumophila* with the same parameters (**Figure 4**).

4. Quantification of polar localization and dynamics of Dot/Icm components

Note: The following steps are designed for images with 0.129 µm per pixel that were acquired with 2 x 2 binning.

4.1. Quantification of polarity for sfGFP fusion proteins (**Figure 5**)

4.1.1. Adjust the image contrast so the bacteria are clearly visible. Use the region tool to place a 0.25 x 1.3 µm rectangle starting at the pole and extending into the cytoplasm. The rectangle must remain precisely within the bacterial borders.

4.1.2. Mark at least 200 bacteria and use the **Region to Mask** button to create masks to the regions of interest. Under **Mask Statistics** and **Mask Scope**, choose **Object**. Then, under **Features** and **Intensity**, mark **Mean Intensity** and **Variance**.

4.1.3. Export the data and calculate the polarity scores of each bacterium as the ratio between the variance to the mean intensity.

4.1.4. For high-throughput applications use a phase objective and an appropriate condenser setup to acquire images with the phase and 488 nm channels. Make sure to choose fields of view where the bacteria are fully separated.

4.1.5. Adjust the phase channel contrast of the image to a level where the bacteria are clearly visible. Open the dual channel image, launch the **Create Segment Mask** window and change the channel to phase.

4.1.6. Adjust an appropriate threshold and remove small objects with the **Define Objects** bottom. Under **Refine Mask** choose **Remove Edges Objects** and later separate masks of bacteria that are adjacent to each other.

4.1.7. Calculate the polarity scores of the signal in the 488 channel for each cell as was previously described in steps 4.1.2–4.1.3.

4.2. Quantification of dynamics for sfGFP fusion proteins (**Figure 6**)

NOTE: Follow the instructions in section 3 to prepare a sample for image acquisition. Dynamics are defined as changes in intensity over time and the following steps are designed for short imaging periods (i.e., several minutes). Add to the pad the appropriate supplements if longer imaging periods are desired.

4.2.1. In the **Image Capture** window, mark **Timelapse**, enter the time of intervals in the interval box, and enter **2** in the **# of Time Points** box. Acquire two successive images of *L. pneumophila* expressing the fluorescent protein of interest.

4.2.2. Adjust the image contrast until the cells are clearly visible. Follow **Figure 6A** and the descriptions below to place three different masks. Use the region tool to place a 0.25 x 0.25 µm square in the middle of at least 400 cells.

4.2.3. Use the **Region to Mask** button to create a mask (mask 1) of the squares of interest. Create a new empty mask (mask 2) and use the pixel tool or the polygon tool to mark the entire cell area of at least 25 random cells, which will be used to calculate fluorescence bleaching. Create a new empty mask (mask 3) and use the large brush tool to mark areas between the cells, which will be used for background subtraction.

4.2.4. Under **Mask Statistics** and **Mask Scope**, choose **Object** for mask 1 and mask 2. Then, under **Features** and **Intensity**, choose **Mean Intensity** and export the data of the two masks. For mask 3, export the mean intensity of the entire mask.

4.2.5. Calculate the change in fluorescence intensity for each object in mask 1 using the following formulas:

$$\text{Bleaching factor} = \bar{X}\,\frac{(\text{mask 2 objects} - \text{mask 3})\text{t1}}{(\text{mask 2 objects} - \text{mask 3})\text{t2}}$$

$$\text{Dynamics}\left[\frac{\text{Intensity change (AU)}}{\text{time}}\right] = \left|1 - \frac{[(\text{mask 1 objects} - \text{mask 3})\text{t2} \times \text{Bleaching factor} \times 100\%]}{(\text{mask 1 objects} - \text{mask 3})\text{t1} \times (\text{t2} - \text{t1})}\right|$$

where mask 1 is a 0.25 µm × 0.25 µm square placed at the cell center, mask 2 covers the whole cell, mask 3 is the background between cells, t1 is the mean intensity in the first time point, and t2 is the mean intensity in the second time point.

5. Detection of sfGFP mass density with cryo-ET

5.1. Sample preparation, data collection, and reconstruction

5.1.1. Grow a heavy patch of *L. pneumophila* expressing a fluorescently tagged Dot/Icm protein on CYE-agar-streptomycin plates for 48 hours at 37 °C. Resuspend the cells in ddH_2O to OD_{600} ~0.7. Add 5 µL of colloidal gold particles (BSA Tracer, 10 nm) to 20 µL of the cell suspension.

5.1.2. Pipette 5 µL of the cell mixture onto freshly glow-discharged holey carbon grid (R 2/1 on Cu 200 mesh) and let stand for 1 min. Blot with filter paper and freeze in liquid ethane using a gravity-driven plunger apparatus as described previously[14,15].

5.1.3. Image the frozen-hydrated specimens with a 300 kV transmission electron microscope equipped with a field emission gun, an energy filter, Volta phase plate, and a direct detection device. Collect single-axis tilt series at 26,000x and 42,000x magnifications, which result in pixel sizes at the specimen level of 5.4 Å/pixel or 3.4 Å/pixel, respectively.

5.1.4. Use the tomographic package SerialEM to collect image stacks at ~0 µm defocus, with a range of tilt angles between -60° and +60° with 3° step increment and accumulative dose of ~60 $e^-/Å^2$[2,16]. Align dose-fractionated movie images in each stack using MotionCor2[17]. Assemble drift-corrected stacks using TOMOAUTO[14].

5.1.5. Align drift-corrected stacks by the IMOD marker-dependent alignment[18]. Reconstruct tomograms with the SIRT method[19] for segmentations and direct image analysis and the WBP method[20].

5.2. Subtomogram analysis of sfGFP fusions samples

5.2.1. Use the tomographic package I3 (0.9.9.3) for subtomogram analysis[14,21,22].

NOTE: The alignment proceeds iteratively, with each iteration consisting of three parts in which references and classification masks are generated, subtomograms are aligned and classified, and class averages are aligned to each other.

Use 4 x 4 x 4 binned subtomograms for an initial alignment. Merge particles that belong to class averages and show electron density corresponding to sfGFP. After sorting particles with sfGFP fusions, use 2 x 2 x 2 binned subtomograms for a focused alignment of a region of interest (like the Dot/Icm cytoplasmic ATPase complex) to obtain a high-resolution structure.

REPRESENTATIVE RESULTS:

Homologous recombination with double selection in two steps was used to construct the defined insertion of sfGFP. In the first step, triparental mating was performed, where the pRK600 conjugative plasmid (an IncP plasmid) from the *E. coli* helper strain MT616 was mobilized to the donor *E. coli* strain with the suicide vector pSR47S containing the sfGFP gene flanked by the two homologous regions, the origin of transfer oriT and the *Bacillus subtilis* counterselection gene *sacB*. Next, the conjugation system from pRK600 assisted mobilization of the pSR47S derivative into *L. pneumophila* (*Lp01*, **Figure 2A**). Clones that successfully integrated pSR47S by a single crossover event were selected due to the antibiotic resistance gene Kan^R and were propagated to allow a second crossover. Clones that lost the *sacB* gene during the second crossover were selected by plating the cells on the counterselective agent sucrose (**Figure 2**, **Figure 3**). Immunoblot analysis with an anti-GFP antibody (α-GFP) was performed to determine whether the sfGFP was cleaved and to assess the stability and expression level of the fusion protein in a wild type or in a complete *dot/icm* deletion mutant. In addition, before proceeding to microscopy, the correct integration of the sfGFP gene into the chromosome was confirmed by PCR (**Figure 3**). Once stability and the integration of the fusions were confirmed, live cell fluorescent microscopy was performed, and specificity of the fluorescent signal clone was compared to a parental sfGFP-negative strain. In addition, dual imaging using bright field or phase microscopy was used to examine the proportion of cells that possessed a specific fluorescent signal (**Figure 4**).

Only a fraction of the cells that produced DotB-sfGFP displayed polar localization of the fusion protein (**Figure 5A**). To characterize the distribution of DotB fluorescence signal, the intensity of DotB-sfGFP along the longitudinal axis in those cells was quantified. DotB intensity at the poles was about 2x higher than in the cytosol (**Figure 5B**). Because it is important to determine whether the localization of fluorescently tagged fusion proteins has biological relevance, we asked if DotB-sfGFP polar localization was dependent on a fully assembled T4BSS. Therefore, polarity scores of DotB-sfGFP indicating the ratio of mean fluorescence measured at the poles compared with fluorescence measured near the middle of the cell were determined for individual cells in a wild type and in a T4BSS mutant (**Figure 5C–E**). Indeed, deletions of the entire Dot/Icm system abrogated polar positioning of DotB-sfGFP, confirming that polar puncta represent association of DotB with the T4SS and the importance of the Dot/Icm machine for recruitment of this ATPase. In most *L. pneumophila* cells, DotB-sfGFP also displayed cytosolic movement, indicating that it is present in a dynamic cytosolic population but is also capable of associating with the polar Dot/Icm complex. To quantify differences in dynamic motion between the DotO and DotB

ATPases, two successive images were acquired and changes in the fluorescence intensity were determined and compared to sfGFP (**Figure 6A**). While sfGFP and DotO-sfGFP showed little to no dynamic patterns, DotB-sfGFP intensity changes in the cytosol were shifted and were significantly higher. These observations indicate that the DotB ATPase was present in a dynamic cytosolic population and at a late-stage assembly reaction, the spatially dynamic DotB ATPase was recruited to the polar-localized Dot/Icm T4SS (**Figure 6B**).

To define the spatial location of DotB relative to the Dot/Icm machine, high-throughput cryo-ET was used to visualize the intact T4BSS apparatus in a *L. pneumophila* strain expressing DotB-sfGFP. First, reconstruction of a *L. pneumophila* cell expressing DotB-sfGFP was performed and revealed typical multiple cone-shaped complexes embedded in the cell envelope (**Figure 7A**, **B**). We demonstrated previously using epistatic experiments with a variety of Dot/Icm mutants, fluorescent microscopy, and cryo-ET that DotB is spatially located below a unique assembly of the ATPase DotO[10]. Subtomogram averaging of the strain expressing DotB-sfGFP determined the overall positioning of DotB in relation to the intact T4BSS machine. This analysis revealed an extra density correlating with the additional mass of sfGFP (**Figure 7C**). Finally, three-dimensional surface renderings of the entire Dot/Icm T4SS indicates that sfGFP is positioned below the DotB hexamer, which assembles as a disc at the base of the cytoplasmic ATPase complex (**Figure 8**)[10].

FIGURE AND TABLE LEGENDS:

Figure 1: Three-dimensional surface renderings of *L. pneumophila* Dot/Icm T4SS. OM = outer membrane, IM = inner membrane, PG = peptidoglycan. The image was modified from Chetrit D. et al.[10].

Figure 2: Schematic overview of homologous recombination and allelic exchange used to insert sfGFP into *L. pneumophila* chromosome. (**A**) Triparental mating performed between an *E. coli* MT616 helper strain that harbors the conjugative plasmid pRK600 (an IncP plasmid), a donor *E. coli* strain that is transformed with the suicide vector pSR47S, and *L. pneumophila* as a recipient. (**B**) Schematic model depicting the steps required to insert sfGFP into the *L. pneumophila* chromosome in order to generate C-terminal sfGFP fusion proteins. Selection of allelic exchange mutants was accomplished in two steps, using kanamycin and the counter selectable marker *sacB*.

Figure 3: The allelic exchange assay workflow. *L. pneumophila* was streaked on the appropriate selections and growths times (see the protocol section for details). Later, insertion of sfGFP into the chromosome was confirmed with colony PCR using primers complementary to the sfGFP gene and to the chromosomal region flanking the insertion site. The stability of the fusion protein was examined by immunoblot analysis using an anti-GFP antibody. Bottom left panels: Lane 1 = untagged *Lp01*, Lane2 = sfGFP expressed from *dotB* operon, Lane 3 = DotB-sfGFP expressed in a complete *dot/icm* deletion mutant, Lane 4 = DotB-sfGFP expressed in a wild type background. WB = western blot. The number of clones analyzed in each step are indicated in parentheses.

Figure 4: Live cell imaging of *L. pneumophila* expressing fluorescently tagged Dot/Icm subunits. (**A**) *L. pneumophila* from a two day heavy patch was resuspended in ddH_2O and placed on top of

1% low melting agarose pads. (**B**) The specificity of the fluorescence signal of a strain that chromosomally encodes DotB-sfGFP was compared to the parental GFP-negative *Lp01* strain. Scale bar = 3 µm.

Figure 5: Quantification of polar localization of Dot/Icm system subunits. (**A**) Real-time visualization of DotB-sfGFP expressed in *Lp01* showed polar localization. DotB-sfGFP displayed a diffuse pattern when expressed in a strain where the entire *dot/icm* gene cluster was deleted (Δ*T4SS*). Unfused sfGFP expressed from the *dotB* operon showed a diffuse cytosolic pattern and served as a control. Scale bar = 3 µm. (**B**) Quantification of DotB-sfGFP fluorescence intensity along the longitudinal axis of cells with polar or diffuse patterns. The samples sizes were n = 20 cells for polar and nonpolar cells. *$p = 0.02$, **$p \leq 0.0001$. The significance was calculated by two-tailed Student`s t-test and compared to the intensity at the pole. (**C**) Schematic model of the masks used to quantify polarity. (**D**) DotB-sfGFP as shown in **Figure 5A** with the masks used to quantify polarity. (**E**) The abundance of DotB-sfGFP at the poles, when it is expressed in a wild type background or when the entire *dot/icm* gene cluster was deleted, is displayed as frequency curves. The samples sizes were $n = 200$ cells for each strain. * $p < 0.0001$. The significance was calculated by two-tailed Mann Whitney test and compared to sfGFP expressed from the *dotB* operon.

Figure 6: Quantification of the dynamics of Dot/Icm fluorescent fusions. (**A**) A schematic model depicting the masks used to quantify the changes in fluorescence intensity for a dynamic or static sfGFP fusion protein. $T_{1,2}$ are the time of the first and second time points and $m_{1,2,3}$ are mask 1, mask 2, and mask 3. (**B**) The dynamics of DotB-sfGFP, DotO-sfGFP, and sfGFP expressed from the *dotB* operon are displayed as frequency curves. The samples sizes were n = 400 cells for each strain. *$p = 3.4 \times 10^{-12}$, ***$p = 1.0 \times 10^{-147}$. The significance was calculated by two-tailed Student`s t-test compared to sfGFP.

Figure 7: Subtomogram averaging is used to determine sfGFP density of DotB-sfGFP. (**A**) A tomographic slice acquired with 26,000x magnification from a representative *L. pneumophila* cell expressing DotB-sfGFP, showing multiple Dot/Icm machines embedded in the cell envelope. (**B**) A tomographic slice acquired with a 42,000x magnification of the same *L. pneumophila* cell pole shown in **A**. OM = outer membrane, IM = inner membrane. (**C**) A reconstruction from a strain expressing DotB-sfGFP shows densities corresponding to DotB and sfGFP (yellow arrows).

Figure 8: Three-dimensional surface renderings of the Dot/Icm cytosolic complex. Three-dimensional surface renderings of the entire Dot-Icm T4SS from Δ*dotB* (**A**), wild type (**B**), and *dotB-gfp* (**C**) *L. pneumophila* strains. (**D**) The structure of the cytosolic complex shows the positioning of DotB (purple) and sfGFP (green). The X-ray structure of DotB (PDB: 6GEB[23]) was docked to the DotB map. IM = inner membrane.

DISCUSSION:

Elucidating the functions of bacterial secretion systems is key to a complete understanding of host-pathogen interactions. Secretion systems are complex machines that can inject effectors proteins into host cells, and in some cases promote establishment of a subcellular niche that

supports bacterial replication. The above method provides important new tools for studying the Dot/Icm secretion system of the respiratory bacterial pathogen *Legionella pneumophila,* yielding clues to the mechanisms of effector translocation that are essential for its pathogenicity. This approach can be applied to other secretion systems by employing live bacterial cell imaging and structural studies to dissect their activity at the molecular level. This can be accomplished by studying the spatiotemporal dynamics of fluorescently tagged secretion system components using time-lapse video microscopy.

We constructed clean and unmarked mutations, where a gene was tagged or replaced by a modified allele, which is a fundamental approach for the understanding of pathogenicity at a molecular level as well as for the definition of structure-function relationships that may lead to the production of drug therapies[24,25]. Strains of *L. pneumophila* that have been genetically modified to eliminate individual Dot and Icm proteins can be used to determine the structure of the Dot/Icm system by cryo-ET. An important step in the protocol is to compare the functionality of N-terminus and C-terminus tagged proteins. Therefore, strains encoding the fusions should be tested for replication in eukaryotic host cells, visualized by microscopy to determine whether tagged protein localization in the bacterial cell is dependent on a fully assembled secretion machine, and assessed for stability of proteins expressed from upstream and downstream genes.

This protocol utilizes live cell microscopy experiments, which are widely used to study complex biological processes such as signal transduction, self-assembly, active trafficking, and gene regulation. Understanding the dynamics, trajectories, and interactions of single particles in cells represents a fundamental approach in cell biology[26]. However, given that tracking single particles may not always be possible due to fast molecular movement or low signal-to-noise ratio, evaluating changes in fluorescence intensity may serve as a straightforward approach to quantify differences in dynamics patterns. In addition, because only two time points are required for the analysis, this methodology guarantees only minimal exposure of the sample to fluorescent light and thus prevents major bleaching of the sfGFP fluorescence intensity. Because the agarose pads do not contain any source of nutrients, it is important to note that live imaging should be performed immediately after taking the cells from the CYE agar plates. If longer periods of imaging time are required, then supplements that support *L. pneumophila* survival and growth should be added to the pads. Determining the polarity of fluorescently tagged proteins can also be modified for high-throughput applications. If these are needed, a phase objective and an appropriate condenser setup should be used to acquire dual channel images (i.e., phase and fluorescent channels). It is crucial to choose fields where the bacteria are fully separated. Use the phase channel to mask entire cells and quantify the ratio of intensities as described above.

Cryo-electron microscopy (cryo-EM) and cryo-ET offer robust visualization of nanoparticles. These techniques involve imaging of the sample in a frozen-hydrated state, allowing visualization of nanoparticles essentially as they exist in their cellular environment[27]. Because resolution is limited by the thickness of the sample, structures obtained by cryo-ET have lower resolution than the ones that are obtained by cryo-EM. Nevertheless, because in each image tomogram type IV machineries are present in multiple copies, increased resolution can be obtained by increasing the sample size for subtomogram averaging. One major advantage of cryo-ET is that visualization

of complex assemblies in intact bacterial cells may better preserve their structure, which can undergo drastic change upon extraction from their natural environment.

In conclusion, the study of dynamic processes and localization of molecules are among the first steps toward understanding the function of biological systems. The strength and focus of the method described here is the direct visualization of Dot/Icm components in living bacteria, which provides the possibility to uncover dynamic processes governing the functions of type IVB machines or other multiprotein assemblies. In addition, coupling live imaging to cryo-ET is a strategy that allows characterization of key components in the Dot/Icm machine in relation to the greater structure of the *Legionella pneumophila* secretion system, and understanding of how they assemble and direct conformational changes in the apparatus. One limitation of fluorescent protein tags used for studying protein behavior in living cells is their relatively large size, which might influence the function and properties of the tagged protein. Subsequently, assessment of stability and functionality is required. Another limitation of this approach is that currently atomic structures cannot be obtained due to the limited resolution resulting from the thickness of the sample. Modeling and fitting can be an effective way to analyze the densities, thus allowing localization of subunits or evaluation of conformational changes. Future investigations and further perfectioning of this approach will lead to a better understanding of how different subassemblies comprise a functional type IV apparatus.

ACKNOWLEDGMENTS:

D.C. and C.R.R. were supported by the NIH (R37AI041699 and R21AI130671). D.P., B.H., and J.L were supported by the National Institutes of Health (R01AI087946 and R01GM107629).

DISCLOSURES:

The authors have nothing to disclose.

REFERENCES:

1. Franco, I. S., Shuman, H. A., Charpentier, X. The perplexing functions and surprising origins of Legionella pneumophila type IV secretion effectors. *Cellular Microbiology*. **11**, 1435–1443 (2009).
2. Burstein, D. et al. Genome-scale identification of Legionella pneumophila effectors using a machine learning approach. *PLOS Pathogens*. **5**, e1000508 (2009).
3. Ninio, S., Roy, C. R. Effector proteins translocated by Legionella pneumophila: strength in numbers. *Trends in Microbiology*. **15**, 372–380 (2007).
4. Vogel, J. P., Andrews, H. L., Wong, S. K., Isberg, R. R. Conjugative transfer by the virulence system of Legionella pneumophila. *Science*. **279**, 873–876 (1998).
5. Isberg, R. R., O'Connor, T. J., Heidtman, M. The Legionella pneumophila replication vacuole: making a cosy niche inside host cells. *Nature Reviews Microbiology*. **7**, 13–24 (2009).
6. Roy, C. R., Berger, K. H., Isberg, R. R. Legionella pneumophila DotA protein is required for early phagosome trafficking decisions that occur within min of bacterial uptake. *Molecular Microbiology*. **28**, 663–674 (1998).
7. Archer, K. A., Roy, C. R. MyD88-Dependent Responses Involving Toll-Like Receptor 2 Are Important for Protection and Clearance of Legionella pneumophila in a Mouse Model of

Legionnaires' Disease 10.1128/IAI.02049-05. *Infection and Immunity*. **74**, 3325–3333 (2006).
8. Nagai, H., Kubori, T. Type IVB Secretion Systems of Legionella and Other Gram-Negative Bacteria. *Frontiers in Microbiology*. **2**, 136 (2011).
9. Kubori, T., Nagai, H. The Type IVB secretion system: an enigmatic chimera. *Current Opinion in Microbiology*. **29**, 22–29 (2016).
10. Chetrit, D., Hu, B., Christie, P. J., Roy, C. R., Liu, J. A unique cytoplasmic ATPase complex defines the Legionella pneumophila type IV secretion channel. *Nature Microbiology*. **3**, 678–686 (2018).
11. Merriam, J. J., Mathur, R., Maxfield-Boumil, R., Isberg, R. R. Analysis of the Legionella pneumophila fliI gene: intracellular growth of a defined mutant defective for flagellum biosynthesis. *Infection and Immunity*. **65**, 2497–2501 (1997).
12. Feeley, J. C. et al. Charcoal-yeast extract agar: primary isolation medium for Legionella pneumophila. *Journal of Clinical Microbiology*. **10**, 437–441 (1979).
13. Andrews, H. L., Vogel, J. P., Isberg, R. R. Identification of linked Legionella pneumophila genes essential for intracellular growth and evasion of the endocytic pathway. *Infection and Immunity*. **66**, 950–958 (1998).
14. Morado, D. R., Hu, B., Liu, J. Using Tomoauto: A Protocol for High-throughput Automated Cryo-electron Tomography. *Journal of Visualized Experiments.* **107**, e53608 (2016).
15. Hu, B., Lara-Tejero, M., Kong, Q., Galan, J. E., Liu, J. In Situ Molecular Architecture of the Salmonella Type III Secretion Machine. *Cell*. **168**, 1065–1074 e1010 (2017).
16. Mastronarde, D. N. Automated electron microscope tomography using robust prediction of specimen movements. *Journal of Structural Biology*. **152**, 36–51 (2005).
17. Zheng, S. Q. et al. MotionCor2: anisotropic correction of beam-induced motion for improved cryo-electron microscopy. *Nature Methods*. **14**, 331–332 (2017).
18. Kremer, J. R., Mastronarde, D. N., McIntosh, J. R. Computer visualization of three-dimensional image data using IMOD. *Journal of Structural Biology*. **116**, 71–76 (1996).
19. Gilbert, P. Iterative methods for the three-dimensional reconstruction of an object from projections. *Journal of Theoretical Biology*. **36**, 105–117 (1972).
20. Radermacher, M. Weighted Back-projection Methods. *Electron Tomography*, pp 245–273 (2007).
21. Winkler, H. et al. Tomographic subvolume alignment and subvolume classification applied to myosin V and SIV envelope spikes. *Journal of Structural Biology*. **165**, 64–77 (2009).
22. Winkler, H., Taylor, K. A. Accurate marker-free alignment with simultaneous geometry determination and reconstruction of tilt series in electron tomography. *Ultramicroscopy*. **106**, 240–254 (2006).
23. Prevost, M. S., Waksman, G. X-ray crystal structures of the type IVb secretion system DotB ATPases. *Protein Science*. **27**, 1464–1475 (2018).
24. Miklos, G. L., Rubin, G. M. The role of the genome project in determining gene function: insights from model organisms. *Cell* **86**, 521–529 (1996).
25. Reyrat, J. M., Pelicic, V., Gicquel, B., Rappuoli, R. Counterselectable markers: untapped tools for bacterial genetics and pathogenesis. *Infection and Immunity*. **66**, 4011–4017 (1998).
26. Yu, J. Single-Molecule Studies in Live Cells. *Annual Review of Physical Chemistry*. **67**, 565–585 (2016).
27. Stewart, P. L. Cryo-electron microscopy and cryo-electron tomography of nanoparticles.

571 *Wiley Interdisciplinary Reviews: Nanomedicine and Nanobiotechnology*. **9**, (2017).
572

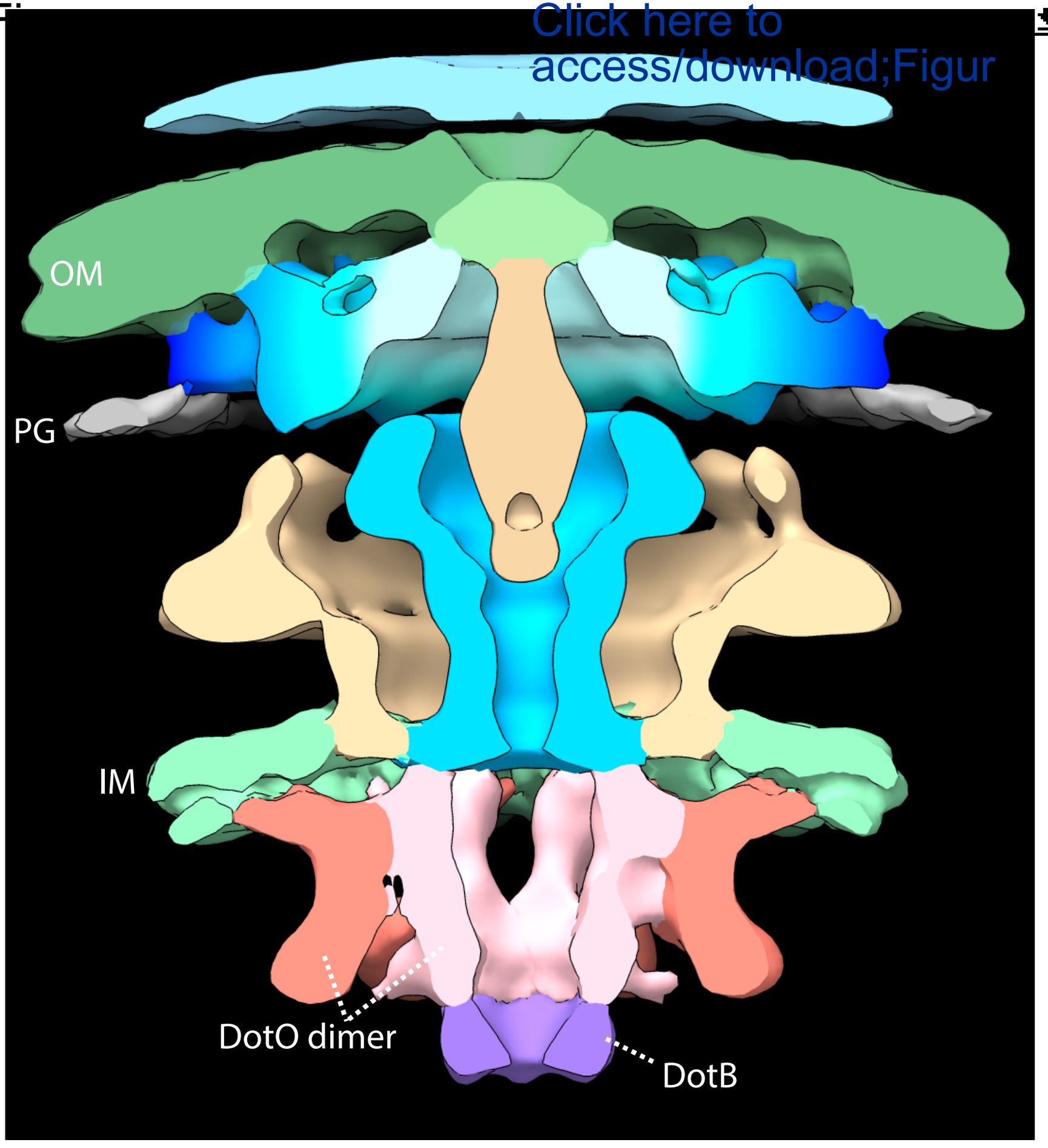

Figure

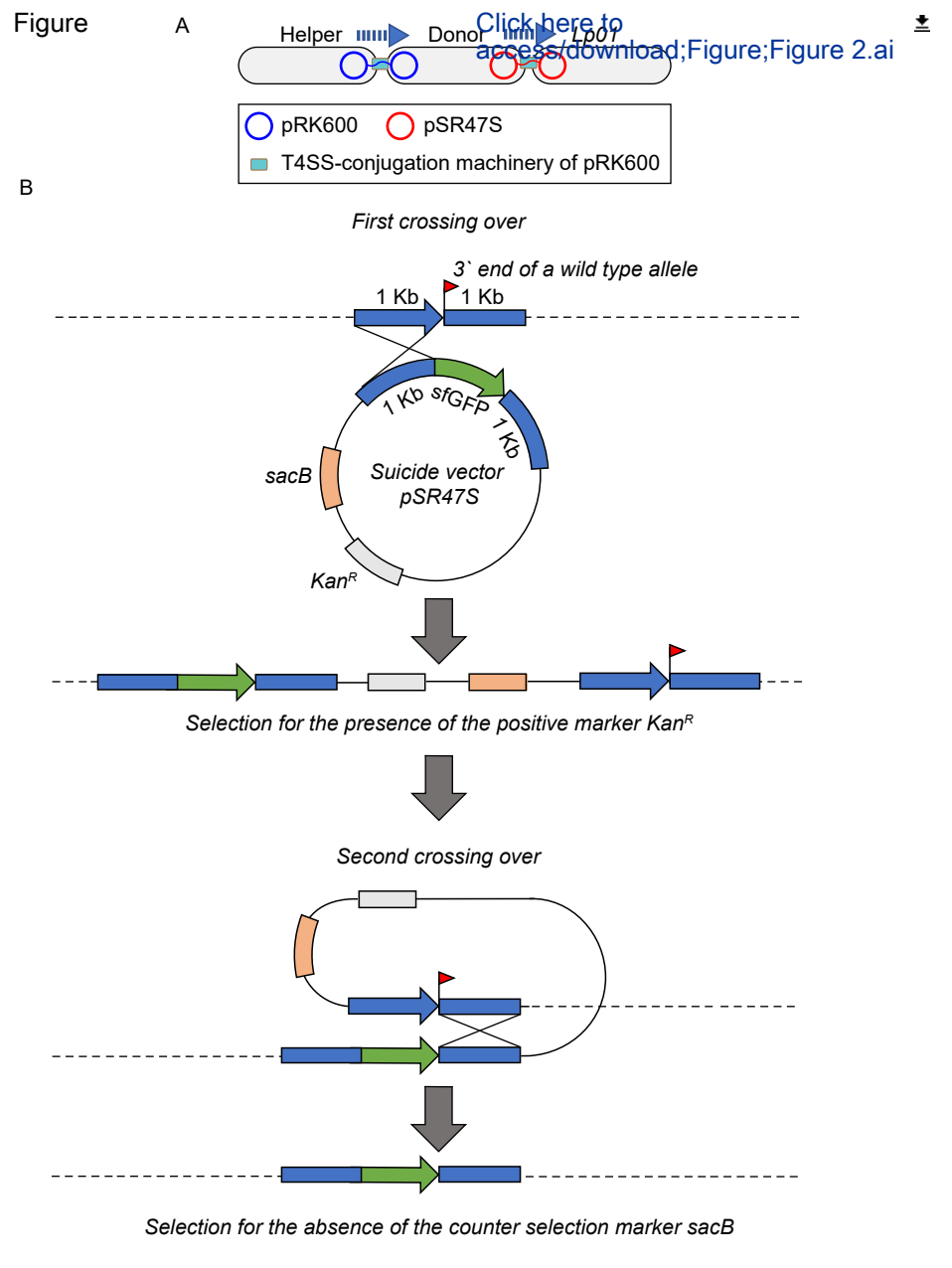

Figure

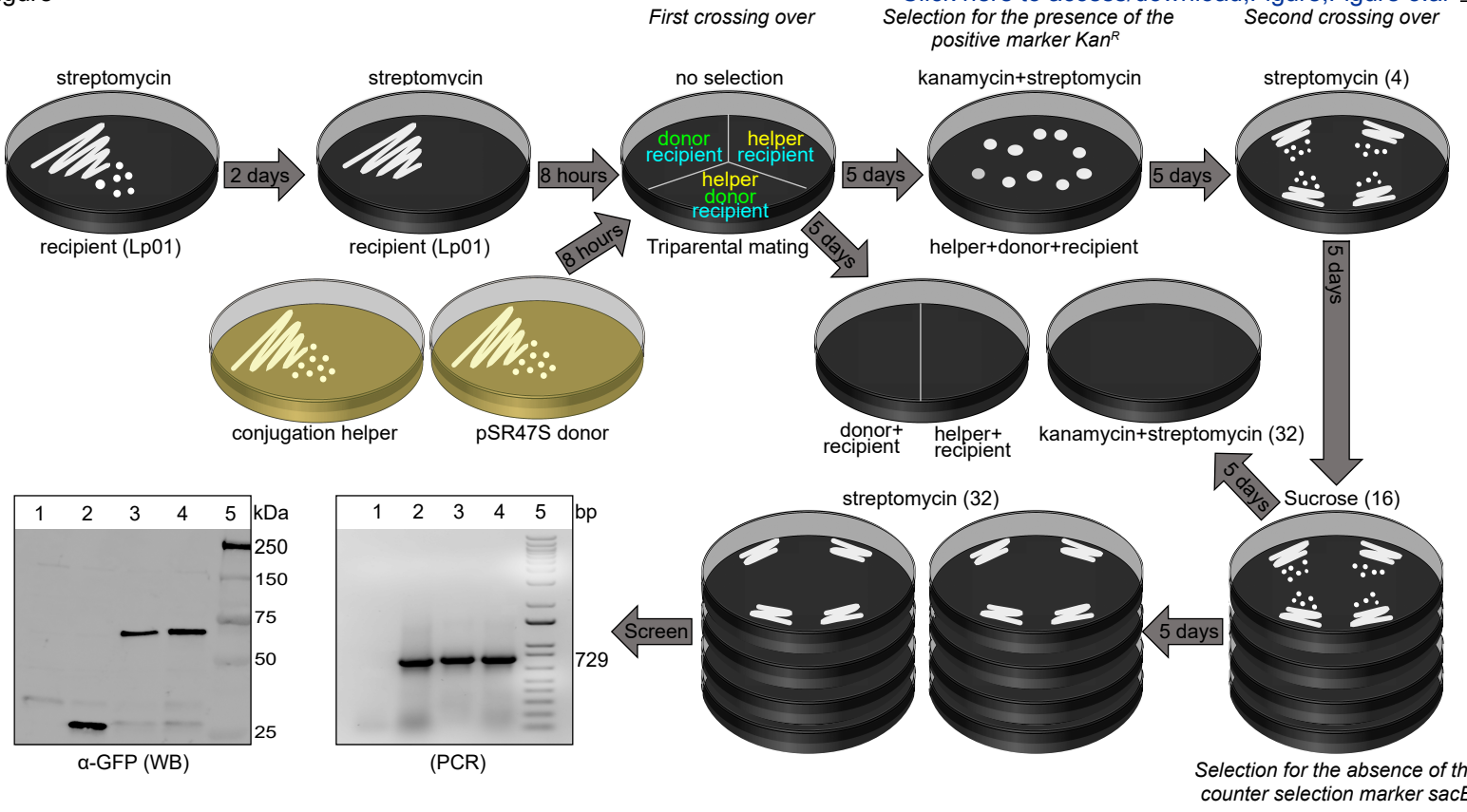

Figure

Click here to access/download;Figure;Figure 4.ai

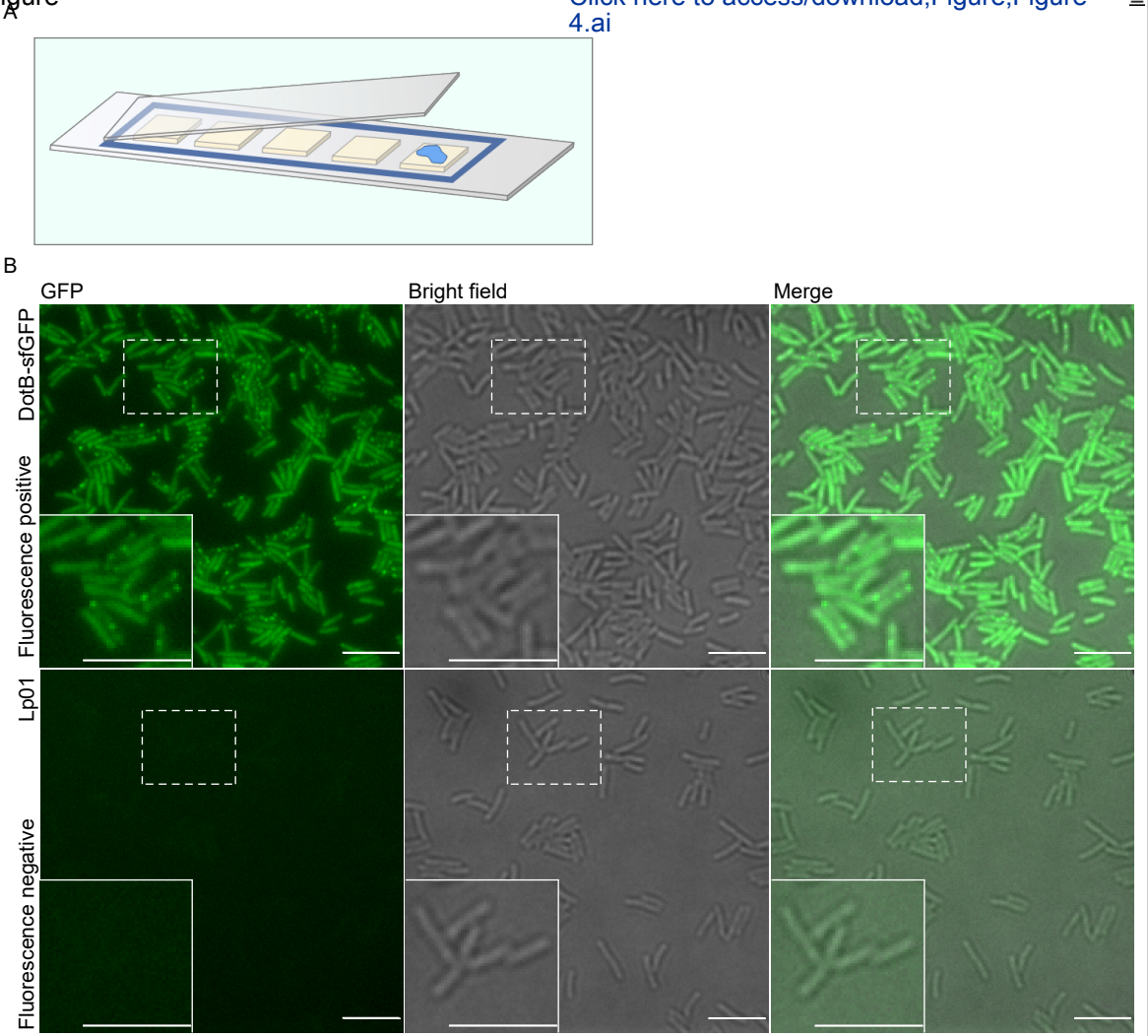

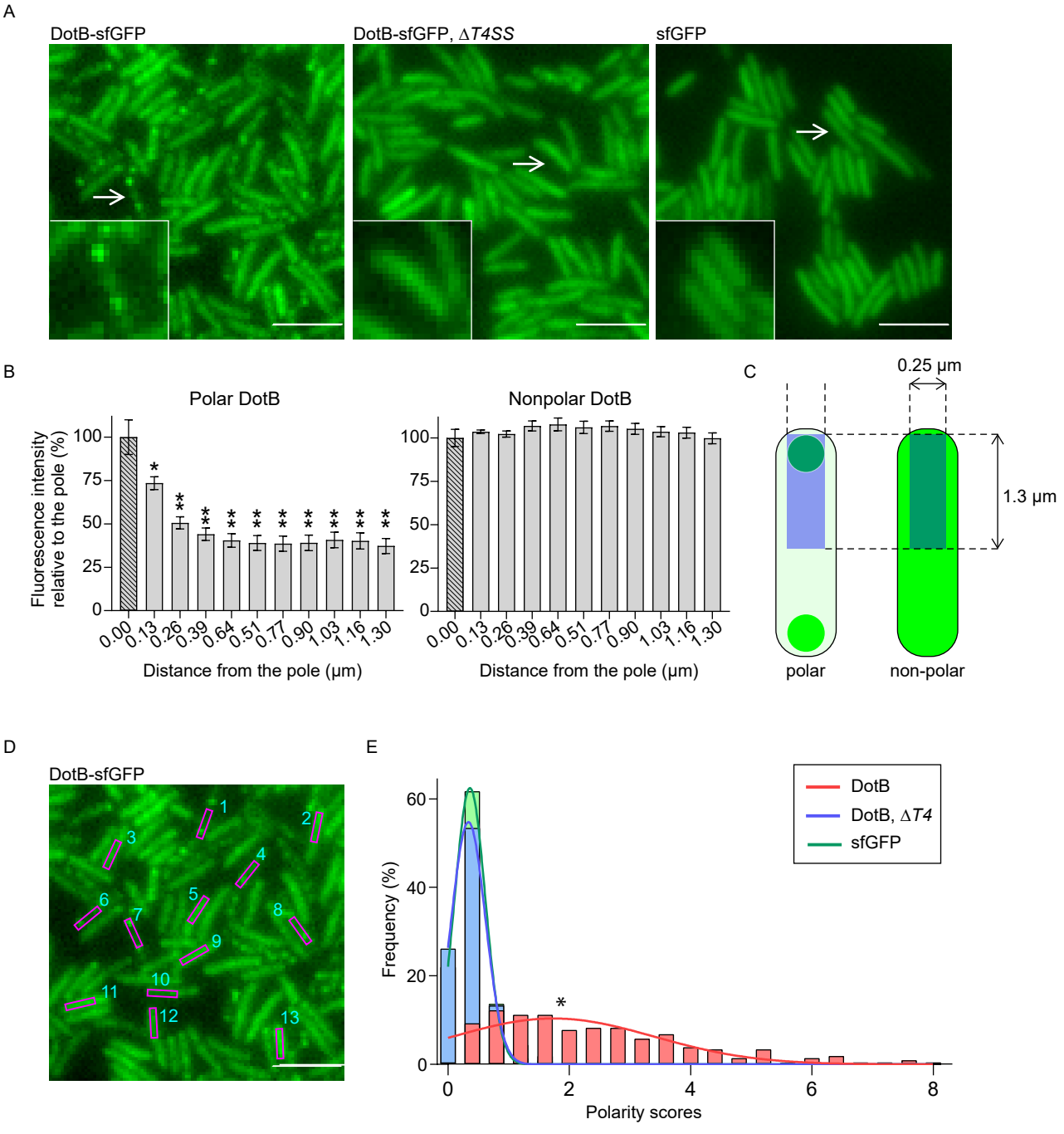
A
DotB-sfGFP
DotB-sfGFP, ΔT4SS
sfGFP
B
Polar DotB
Nonpolar DotB
Fluorescence intensity relative to the pole (%)
100
75
50
25
0
0.00
0.13
0.26
0.39
0.64
0.51
0.77
0.90
1.03
1.16
1.30
Distance from the pole (μm)
C
0.25 μm
1.3 μm
polar
non-polar
D
DotB-sfGFP
1
2
3
4
5
6
7
8
9
10
11
12
13
E
DotB
DotB, ΔT4
sfGFP
Frequency (%)
60
40
20
0
0
2
4
6
8
Polarity scores

Figure

Click here to access/download;Figure;Figure 6.ai

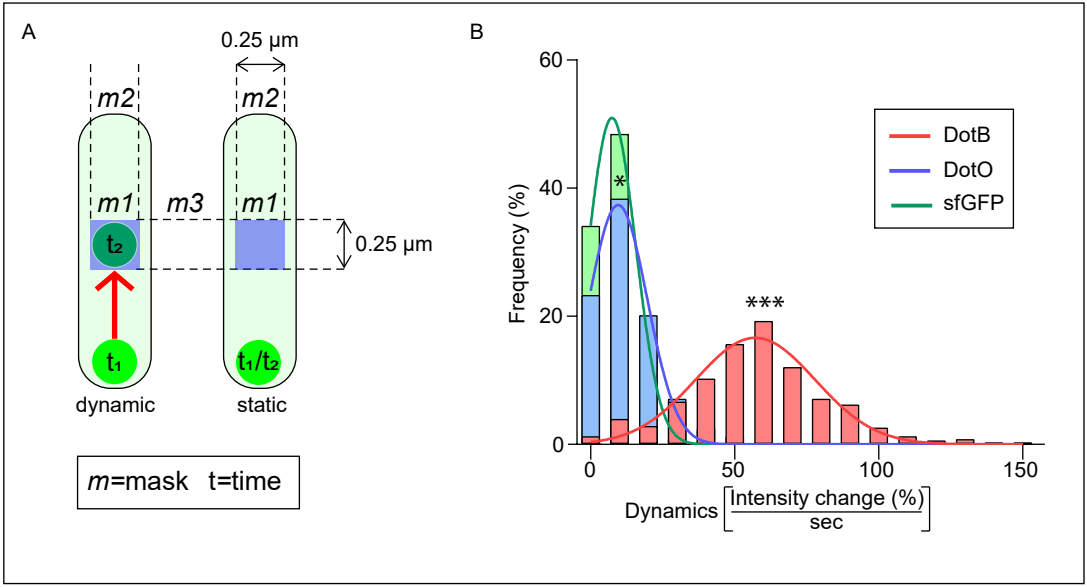

Figure

Click here to access/download;Figure;Figure 7.ai

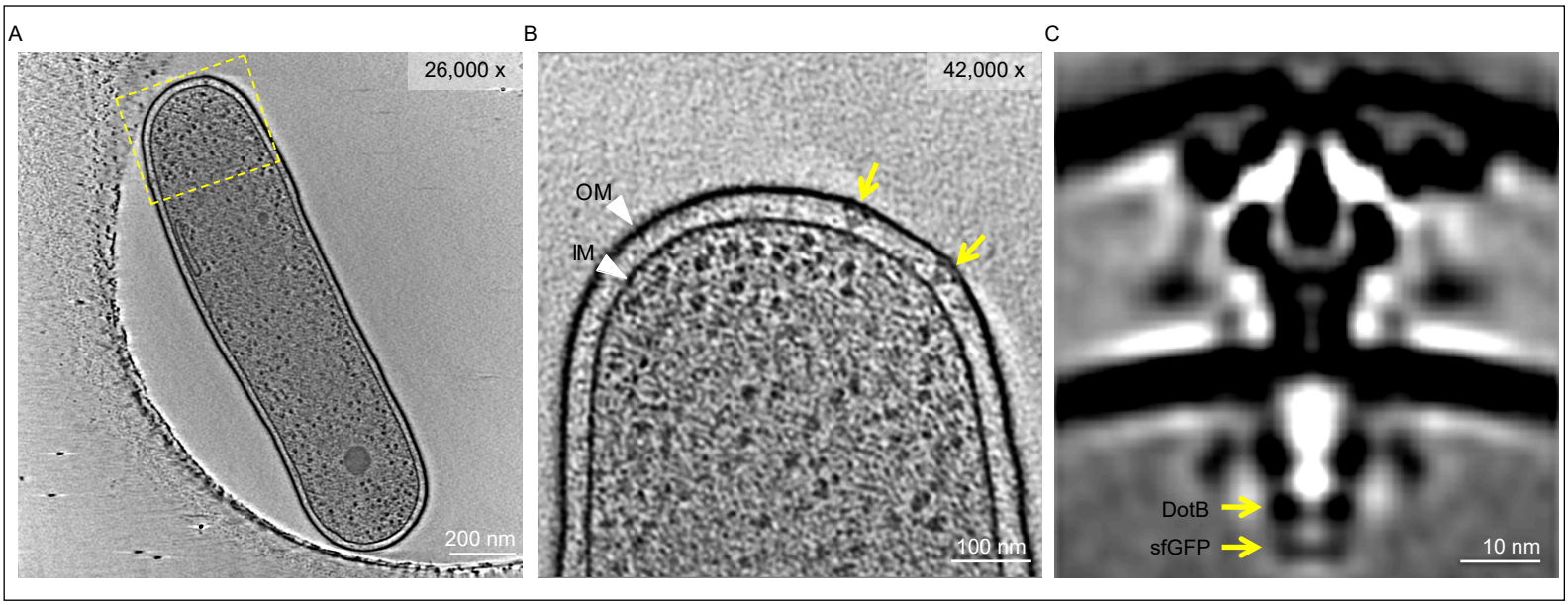

Figure

Click here to access/download;Figure;Figure 8.ai

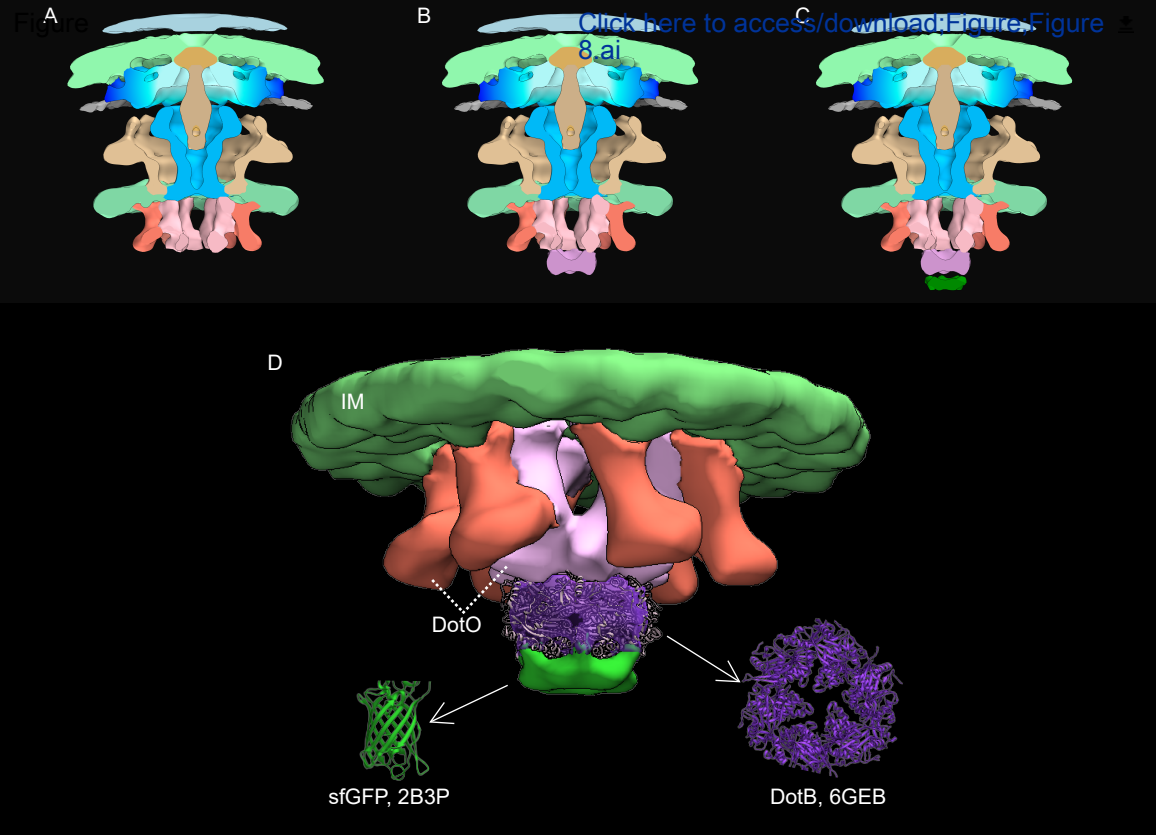

Table of Materials

Name of Material/ Equipment	Company	Catalog Number	Comments/Description
10 nm colloidal gold particles	Aurion	25486	
100x Plan Apo objective (1.4 NA)	Nikon		
ACES	Sigma-Aldrich	A9758	
Activated charcoal	Sigma-Aldrich	C5510	
Agaroze GPG/LMP, low melt	American bioanalytical	AB00981	
Bacto dehydrated agar	BD	214010	
CoolSNAP EZ 20 MHz digital monochrome camera	Photometrics		
Gene Frame, 1.7x2.8 cm, 125 µL	Fisher Scientific	AB-0578	
Holey Carbon grid R 2/1 Cu 200 mesh	Quantifoil	Q225-CR1	
Iron(III) nitrate nonahydrate	Sigma-Aldrich	216828	
K2 Summit camera for cryo-EM	GATAN		
L-Cysteine	Sigma-Aldrich	C7352	
Microscope cover slides 22x22 mm	Fisher Scientific	12-542B	
Microscope cover slides 24x50 mm	Fisher Scientific	12-545K	
Microscope slides 25x75x1 mm	Globe scientific	1380	
SlideBook 6.0	Intelligent Imaging Innovations		
Spectra X light engine	Lumencor		
Taq 2X Master Mix	New England BioLabs	M0270	
Titan Krios	Thermo fisher scientific		
Yeast Extract	BD	212750	

Editorial comments:

General:

1. Please take this opportunity to thoroughly proofread the manuscript to ensure that there are no spelling or grammar issues.

We have reviewed the manuscript and changed the wording where appropriate.

2. Please capitalize the 'L' in 'mL' and 'µL'.

We have capitalized the 'L' where appropriate.

3. Please include at least 6 key words or phrases.

We have included 14 key words and phrases.

4. Please remove references from the summary (and renumber accordingly).

We have removed references from the summery and renumbered the citations accordingly.

5. JoVE cannot publish manuscripts containing commercial language. This includes trademark symbols (™), registered symbols (®), and company names before an instrument or reagent. Please limit the use of commercial language from your manuscript and use generic terms instead. All commercial products should be sufficiently referenced in the Table of Materials and Reagents. For example: SlideBook, Spectra X, CoolSNAP, Nikon Plan, Titan Krios

We have removed Spectra X, CoolSNAP, Nikon Plan, Titan Krios from the protocol and updated the table of materials and reagents. We have kept SlideBook in the protocol section as we wish that SlideBook will be used as a model for other users, which we believe will allow easy adaptation into different acquiring and analysis software. We would be happy to remove SlideBook from the protocol section if the editor feels it is important.

Protocol:

For each step/substep, please ensure you answer the "how" question, i.e., how is the step performed? Alternatively, add references to published material specifying how to perform the protocol action. If revisions cause a step to have more than 2-3 actions and 4 sentences per step, please split into separate steps or substeps.

We have tried to make the protocol clear by changing the wording in the protocol.

Figures:

1. Please obtain explicit copyright permission to reuse any figures from a previous publication. Explicit permission can be expressed in the form of a letter from the editor or a link to the editorial policy that allows re-prints. Please upload this information as a .doc or .docx file to your Editorial Manager account.

We have uploaded a document that include a link to Nature editorial policy that allows re-prints by the authors.

2. Figure 4: Please define the scale bars here.

We have defined the scare bar as requested.

References:

Please do not abbreviate journal titles.

We have included the full journal titles as requested.

Table of Materials:

Please ensure the Table of Materials has information on all materials and equipment used, especially those mentioned in the Protocol.

We have updated the table of materials with all the information and equipment as requested.

****

Reviewers' comments:

Reviewer #1 (Remarks to the Author):

Manuscript Summary: The manuscript by Chetrit et al. describes the use of fluorescence microscopy and cryo-ET to study the architecture and localization of the type IV secretion system machinery. The manuscript is very clearly written and easy to follow. The sections follow a logical order and the figures are clear. Some information may be given somewhat more detailed (see below). The description of this method should be of use to researchers in the field of bacterial secretion systems, not only of type IV secretion.

We thank the reviewer for the positive evaluation. As suggested, we changed the wording in the abstract and described the method as suitable for researchers in the field of bacterial secretion systems.

Major Concerns:

None.

Minor Concerns:

Some sentences are a bit long and may be shortened, e.g. line 99 (II).

We have reviewed the manuscript and changed the wording where appropriate.

The "degree" sign when indicating temperatures is a superscript "0" but should be a true "degree" circle "°".

As suggested, we replaced the “0” with degree circles.

Line 120: Specify where to place GFP: C-terminal, N-terminal, in frame of course. What is best, what does the experience say regarding the functionality of the fusion proteins?

We have changed the protocol as suggested. Based on our experience with the Dot/Icm system we prefer to use an experimental approach to determine where to place the GFP. To address this question we explain in the discussion section that it is important to tag both the N-terminus and C-terminus and compare the fusions functionality in various assays.

Line 149: Specify details of "colony PCR". Is there anything special? How do you prepare the colony for PCR, how much is added to the reaction?

We have reviewed the protocol and changed the wording where appropriate.

Line 184: What is a "heavy patch"? Better term, maybe "thick"? Also in line 268.

In section 1.2 we define “heavy patch” as 2 days growth of *L. pneumophila* on CYE plate. The term was commonly used in by several Roy lab papers and we added a citation that refer to our latest Nature-Micro paper where the term was used.

Line 184: Specify volume of ddH2O. Is it the same as in Line 269?

We have specified the volume in line 184 as suggested. In line 269 the cells are resuspended into an OD600 ~ 0.7. Here there is no need to define a volume since in the next sentence 20 µl cell suspension are mixed with 5 µl colloidal gold particles.

****

Reviewer #2:

Manuscript Summary: In this nicely written technical procedure, Chetrit et al described a stepwise protocol of a method that integrates live cell imaging and Cryo-Electron Tomography to visualize large protein complexes in bacterial cells. Using visualization of the Dot/Icm transporter of Legionella pneumophila as an example, the authors provided very clear experimental procedures than ranges from the construction of bacterial strains that expressed GFP fusions of genes expressed from their endogenous promoters and subsequent sample preparation. The detailed description will allow new users to perform similar experiments without much trouble. The manuscript is well written and easy to follow, I have only a few minor points for the authors to consider.

We thank the reviewer for the suggestions and positive feedback.

Major Concerns:

None.

Minor Concerns:

1. In the last paragraph of discussion, some limitations of the described methods should be discussed.

We have added at the last paragraph of the discussion some limitations of the describe method as suggested.

2. Line 64 Should "T4BSS" be "T4BSSs"?

We have changed the wording as suggested.

3. Line 65, delete "other" before "bacterial".

We have changed the wording as suggested.

4. Line 72, "showed"?

We have changed into “showed” as suggested.

5. Line 106 "membranes".

We believe “membrane” is grammatically correct because it describes the singular form of membrane surrounding the cytoplasm of a cell, however, if we are wrong this will be corrected.

1. Link to Nature editorial policy that allows re-prints by the authors.

   https://www.nature.com/nature-research/reprints-and-permissions/permissions-requests

2. The editorial policy as shown in Nature web site.

Get permission to reuse Springer Nature content online

Permission requests from authors

The author of articles published by Springer Nature do not usually need to seek permission for re-use of their material as long as the journal is credited with initial publication.

Ownership of copyright in in original research articles remains with the Author, and provided that, when reproducing the contribution or extracts from it or from the Supplementary Information, the Author acknowledges first and reference publication in the Journal, the Author retains the following non-exclusive rights:

To reproduce the contribution in whole or in part in any printed volume (book or thesis) of which they are the author(s).

The author and any academic institution where they work at the time may reproduce the contribution for the purpose of course teaching.

To reuse figures or tables created by the Author and contained in the Contribution in oral presentations and other works created by them.

To post a copy of the contribution as accepted for publication after peer review (in locked Word processing file, of a PDF version thereof) on the Author's own web site, or the Author's institutional repository, or the Author's funding body's archive, six months after publication of the printed or online edition of the Journal, provided that they also link to the contribution on the publisher's website.

The above use of the term 'Contribution' refers to the author's own version, not the final version as published in the Journal.

1 Alewife Center #200
Cambridge, MA 02140
tel. 617.945.9051
www.jove.com

ARTICLE AND VIDEO LICENSE AGREEMENT

Title of Article:	Applying Live Cell Imaging and Cryo Electron Tomography to Resolve Spatiotemporal Characteristics of Legionella pneumonia Dot/Icm Secretion System
Author(s):	David Chetrit, Donghyun Park, Bo Hu, Jun Liu, Craig R. Roy

Item 1: The Author elects to have the Materials be made available (as described at http://www.jove.com/publish) via:

☑ Standard Access ☐ Open Access

Item 2: Please select one of the following items:

☑ The Author is **NOT** a United States government employee.

☐ The Author is a United States government employee and the Materials were prepared in the course of his or her duties as a United States government employee.

☐ The Author is a United States government employee but the Materials were NOT prepared in the course of his or her duties as a United States government employee.

ARTICLE AND VIDEO LICENSE AGREEMENT

1. **Defined Terms.** As used in this Article and Video License Agreement, the following terms shall have the following meanings: "**Agreement**" means this Article and Video License Agreement; "**Article**" means the article specified on the last page of this Agreement, including any associated materials such as texts, figures, tables, artwork, abstracts, or summaries contained therein; "**Author**" means the author who is a signatory to this Agreement; "**Collective Work**" means a work, such as a periodical issue, anthology or encyclopedia, in which the Materials in their entirety in unmodified form, along with a number of other contributions, constituting separate and independent works in themselves, are assembled into a collective whole; "**CRC License**" means the Creative Commons Attribution-Non Commercial-No Derivs 3.0 Unported Agreement, the terms and conditions of which can be found at: http://creativecommons.org/licenses/by-nc-nd/3.0/legalcode; "**Derivative Work**" means a work based upon the Materials or upon the Materials and other pre-existing works, such as a translation, musical arrangement, dramatization, fictionalization, motion picture version, sound recording, art reproduction, abridgment, condensation, or any other form in which the Materials may be recast, transformed, or adapted; "**Institution**" means the institution, listed on the last page of this Agreement, by which the Author was employed at the time of the creation of the Materials; "**JoVE**" means MyJove Corporation, a Massachusetts corporation and the publisher of The Journal of Visualized Experiments; "**Materials**" means the Article and / or the Video; "**Parties**" means the Author and JoVE; "**Video**" means any video(s) made by the Author, alone or in conjunction with any other parties, or by JoVE or its affiliates or agents, individually or in collaboration with the Author or any other parties, incorporating all or any portion of the Article, and in which the Author may or may not appear.

2. **Background.** The Author, who is the author of the Article, in order to ensure the dissemination and protection of the Article, desires to have the JoVE publish the Article and create and transmit videos based on the Article. In furtherance of such goals, the Parties desire to memorialize in this Agreement the respective rights of each Party in and to the Article and the Video.

3. **Grant of Rights in Article.** In consideration of JoVE agreeing to publish the Article, the Author hereby grants to JoVE, subject to **Sections 4** and **7** below, the exclusive, royalty-free, perpetual (for the full term of copyright in the Article, including any extensions thereto) license (a) to publish, reproduce, distribute, display and store the Article in all forms, formats and media whether now known or hereafter developed (including without limitation in print, digital and electronic form) throughout the world, (b) to translate the Article into other languages, create adaptations, summaries or extracts of the Article or other Derivative Works (including, without limitation, the Video) or Collective Works based on all or any portion of the Article and exercise all of the rights set forth in (a) above in such translations, adaptations, summaries, extracts, Derivative Works or Collective Works and(c) to license others to do any or all of the above. The foregoing rights may be exercised in all media and formats, whether now known or hereafter devised, and include the right to make such modifications as are technically necessary to exercise the rights in other media and formats. If the "Open Access" box has been checked in **Item 1** above, JoVE and the Author hereby grant to the public all such rights in the Article as provided in, but subject to all limitations and requirements set forth in, the CRC License.

4. **Retention of Rights in Article.** Notwithstanding the exclusive license granted to JoVE in **Section 3** above, the Author shall, with respect to the Article, retain the non-exclusive right to use all or part of the Article for the non-commercial purpose of giving lectures, presentations or teaching classes, and to post a copy of the Article on the Institution's website or the Author's personal website, in each case provided that a link to the Article on the JoVE website is provided and notice of JoVE's copyright in the Article is included. All non-copyright intellectual property rights in and to the Article, such as patent rights, shall remain with the Author.

5. **Grant of Rights in Video – Standard Access.** This **Section 5** applies if the "Standard Access" box has been checked in **Item 1** above or if no box has been checked in **Item 1** above. In consideration of JoVE agreeing to produce, display or otherwise assist with the Video, the Author hereby acknowledges and agrees that, Subject to **Section 7** below, JoVE is and shall be the sole and exclusive owner of all rights of any nature, including, without limitation, all copyrights, in and to the Video. To the extent that, by law, the Author is deemed, now or at any time in the future, to have any rights of any nature in or to the Video, the Author hereby disclaims all such rights and transfers all such rights to JoVE.

6. **Grant of Rights in Video – Open Access.** This **Section 6** applies only if the "Open Access" box has been checked in **Item 1** above. In consideration of JoVE agreeing to produce, display or otherwise assist with the Video, the Author hereby grants to JoVE, subject to **Section 7** below, the exclusive, royalty-free, perpetual (for the full term of copyright in the Article, including any extensions thereto) license (a) to publish, reproduce, distribute, display and store the Video in all forms, formats and media whether now known or hereafter developed (including without limitation in print, digital and electronic form) throughout the world, (b) to translate the Video into other languages, create adaptations, summaries or extracts of the Video or other Derivative Works or Collective Works based on all or any portion of the Video and exercise all of the rights set forth in (a) above in such translations, adaptations, summaries, extracts, Derivative Works or Collective Works and (c) to license others to do any or all of the above. The foregoing rights may be exercised in all media and formats, whether now known or hereafter devised, and include the right to make such modifications as are technically necessary to exercise the rights in other media and formats. For any Video to which this **Section 6** is applicable, JoVE and the Author hereby grant to the public all such rights in the Video as provided in, but subject to all limitations and requirements set forth in, the CRC License.

7. **Government Employees.** If the Author is a United States government employee and the Article was prepared in the course of his or her duties as a United States government employee, as indicated in **Item 2** above, and any of the licenses or grants granted by the Author hereunder exceed the scope of the 17 U.S.C. 403, then the rights granted hereunder shall be limited to the maximum rights permitted under such statute. In such case, all provisions contained herein that are not in conflict with such statute shall remain in full force and effect, and all provisions contained herein that do so conflict shall be deemed to be amended so as to provide to JoVE the maximum rights permissible within such statute.

8. **Protection of the Work.** The Author(s) authorize JoVE to take steps in the Author(s) name and on their behalf if JoVE believes some third party could be infringing or might infringe the copyright of either the Author's Article and/or Video.

9. **Likeness, Privacy, Personality.** The Author hereby grants JoVE the right to use the Author's name, voice, likeness, picture, photograph, image, biography and performance in any way, commercial or otherwise, in connection with the Materials and the sale, promotion and distribution thereof. The Author hereby waives any and all rights he or she may have, relating to his or her appearance in the Video or otherwise relating to the Materials, under all applicable privacy, likeness, personality or similar laws.

10. **Author Warranties.** The Author represents and warrants that the Article is original, that it has not been published, that the copyright interest is owned by the Author (or, if more than one author is listed at the beginning of this Agreement, by such authors collectively) and has not been assigned, licensed, or otherwise transferred to any other party. The Author represents and warrants that the author(s) listed at the top of this Agreement are the only authors of the Materials. If more than one author is listed at the top of this Agreement and if any such author has not entered into a separate Article and Video License Agreement with JoVE relating to the Materials, the Author represents and warrants that the Author has been authorized by each of the other such authors to execute this Agreement on his or her behalf and to bind him or her with respect to the terms of this Agreement as if each of them had been a party hereto as an Author. The Author warrants that the use, reproduction, distribution, public or private performance or display, and/or modification of all or any portion of the Materials does not and will not violate, infringe and/or misappropriate the patent, trademark, intellectual property or other rights of any third party. The Author represents and warrants that it has and will continue to comply with all government, institutional and other regulations, including, without limitation all institutional, laboratory, hospital, ethical, human and animal treatment, privacy, and all other rules, regulations, laws, procedures or guidelines, applicable to the Materials, and that all research involving human and animal subjects has been approved by the Author's relevant institutional review board.

11. **JoVE Discretion.** If the Author requests the assistance of JoVE in producing the Video in the Author's facility, the Author shall ensure that the presence of JoVE employees, agents or independent contractors is in accordance with the relevant regulations of the Author's institution. If more than one author is listed at the beginning of this Agreement, JoVE may, in its sole

jove JOURNAL OF VISUALIZED EXPERIMENTS
1 Alewife Center #200
Cambridge, MA 02140
tel. 617.945.9051
www.jove.com

ARTICLE AND VIDEO LICENSE AGREEMENT

discretion, elect not take any action with respect to the Article until such time as it has received complete, executed Article and Video License Agreements from each such author. JoVE reserves the right, in its absolute and sole discretion and without giving any reason therefore, to accept or decline any work submitted to JoVE. JoVE and its employees, agents and independent contractors shall have full, unfettered access to the facilities of the Author or of the Author's institution as necessary to make the Video, whether actually published or not. JoVE has sole discretion as to the method of making and publishing the Materials, including, without limitation, to all decisions regarding editing, lighting, filming, timing of publication, if any, length, quality, content and the like.

12. **Indemnification.** The Author agrees to indemnify JoVE and/or its successors and assigns from and against any and all claims, costs, and expenses, including attorney's fees, arising out of any breach of any warranty or other representations contained herein. The Author further agrees to indemnify and hold harmless JoVE from and against any and all claims, costs, and expenses, including attorney's fees, resulting from the breach by the Author of any representation or warranty contained herein or from allegations or instances of violation of intellectual property rights, damage to the Author's or the Author's institution's facilities, fraud, libel, defamation, research, equipment, experiments, property damage, personal injury, violations of institutional, laboratory, hospital, ethical, human and animal treatment, privacy or other rules, regulations, laws, procedures or guidelines, liabilities and other losses or damages related in any way to the submission of work to JoVE, making of videos by JoVE, or publication in JoVE or elsewhere by JoVE. The Author shall be responsible for, and shall hold JoVE harmless from, damages caused by lack of sterilization, lack of cleanliness or by contamination due to the making of a video by JoVE its employees, agents or independent contractors. All sterilization, cleanliness or decontamination procedures shall be solely the responsibility of the Author and shall be undertaken at the Author's expense. All indemnifications provided herein shall include JoVE's attorney's fees and costs related to said losses or damages. Such indemnification and holding harmless shall include such losses or damages incurred by, or in connection with, acts or omissions of JoVE, its employees, agents or independent contractors.

13. **Fees.** To cover the cost incurred for publication, JoVE must receive payment before production and publication of the Materials. Payment is due in 21 days of invoice. Should the Materials not be published due to an editorial or production decision, these funds will be returned to the Author. Withdrawal by the Author of any submitted Materials after final peer review approval will result in a US$1,200 fee to cover pre-production expenses incurred by JoVE. If payment is not received by the completion of filming, production and publication of the Materials will be suspended until payment is received.

14. **Transfer, Governing Law.** This Agreement may be assigned by JoVE and shall inure to the benefits of any of JoVE's successors and assignees. This Agreement shall be governed and construed by the internal laws of the Commonwealth of Massachusetts without giving effect to any conflict of law provision thereunder. This Agreement may be executed in counterparts, each of which shall be deemed an original, but all of which together shall be deemed to me one and the same agreement. A signed copy of this Agreement delivered by facsimile, e-mail or other means of electronic transmission shall be deemed to have the same legal effect as delivery of an original signed copy of this Agreement.

A signed copy of this document must be sent with all new submissions. Only one Agreement is required per submission.

CORRESPONDING AUTHOR

Name:	David Chetrit
Department:	Department of Microbial Pathogenesis
Institution:	Yale School of Medicine
Title:	Associate research scientist
Signature:	David Chetrit
Date:	8/19/2019

Please submit a **signed** and **dated** copy of this license by one of the following three methods:

1. Upload an electronic version on the JoVE submission site
2. Fax the document to +1.866.381.2236
3. Mail the document to JoVE / Attn: JoVE Editorial / 1 Alewife Center #200 / Cambridge, MA 02140